The 2009 IEEE/RSJ International Conference on
Intelligent Robots and Systems
October 11-15, 2009 St. Louis, USA

VPass: Algorithmic Compass using Vanishing Points in Indoor Environments

Young Hoon Lee, Changjoo Nam, Keon Yong Lee, Yuen Shang Li, Soo Yong Yeon, and Nakju Lett Doh

***Abstract*— In this paper, we propose an algorithmic compass that yields the heading information of a mobile robot using the vanishing point in indoor environments: VPass. With the VPass, a loop-closing effect (which is a significant reduction of errors by revisiting a known place through a loop) can be achieved even for a loop-less environment. From the implementation point of view, the VPass is useful because it can be appended upon any existing navigation algorithms. Experimental results show that the VPass yields accurate angle information in indoor environments for paths with lengths of around $200m$.**

I. INTRODUCTION

In this paper, we propose an algorithmic compass that yields accurate heading information of mobile robots. To explain the physical meaning of our approach, let us assume that there exist two landmarks attached to the ceiling of a building (Fig. 1) and a mobile robot can detect them in the building. Then the size of covariance matrix is bounded within degrees of sensing errors (ellipse around the robot in Fig. 1), and navigation problems such as localization, SLAM, and the integrated exploration become more tractable.

We denote this kind of landmark as '*an absolute landmark*' which has the following characteristics. First, it should be detected at every place (omni-presence). Second, it should be accurately detected (high accuracy). Third, it should be distinctive to prevent a false data-association (sparseness).

However, there is no such a landmark in indoor environments. Thus previous researches have tried to reduce localization errors through the following three approaches.

First, researchers have suppressed an error growth rate. For example, odometry calibration was performed in [1] because an uncalibrated odometry is a main source of the error growth. Some researchers utilized a high-performance sensors (such as laser scanners) to reduce the sensing errors. One of methods is to gaze on one landmark as long as possible because the error is bounded by the uncertainty of that landmark. Recently, the unscented transformation [2] has been used to decrease the linearization error which is a major reason of the error growth in an algorithmic point of view.

Yet, These relative localization approaches have weakness that the errors are apt to be accumulated as the robot moves. For example, an angle error occurred at point A in Fig. 2(b) increases errors as the robot moves.

Second, researchers have used a loop-closing technique [3] by visiting the same place twice and this technique decreased the error of the second visit to that of the first visit. However if there is no loop, this method cannot be applied for.

All authors are with the School of Engineering, Korea University, Seoul, KOREA, Fax: +82-2-3290-3666. All correspondence should be addressed to nakju@korea.ac.kr.

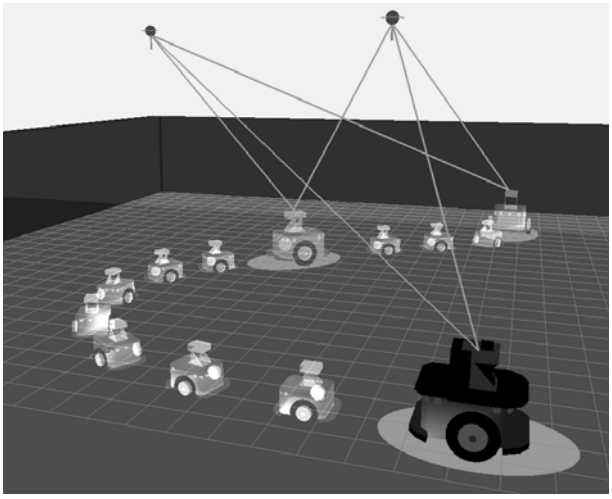

Fig. 1. Physical meaning of an absolute landmark.

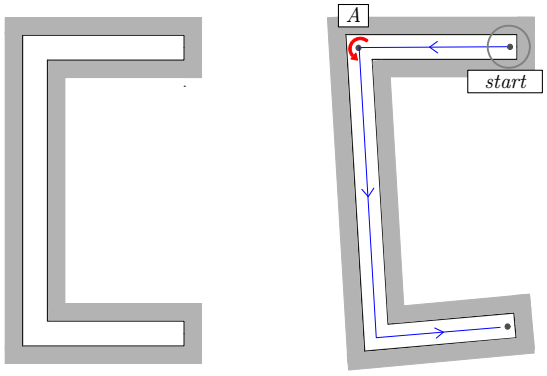

(a) (b)

Fig. 2. For a given map in (a), an angle error occurred at point A in (b) increases errors as the robot moves.

Third, some researchers have added a geometric constraint such as orthogonality [4], [5]. This method shows good performance but there are two weaknesses: it cannot be applied to an environment without orthogonality as shown in (Fig. 4(a)) and the constraint cannot be generated automatically.

In this paper, we propose an algorithmic compass that works as virtual absolute landmarks in indoor buildings: a VPass (Vanishing point based comPass). It is based on an idea that vanishing point (VP in short) of corridors in the same direction is mapped into the same point by a projective transformation. For example, let us apply a projective transformation to a loop-less map (thus the loop-

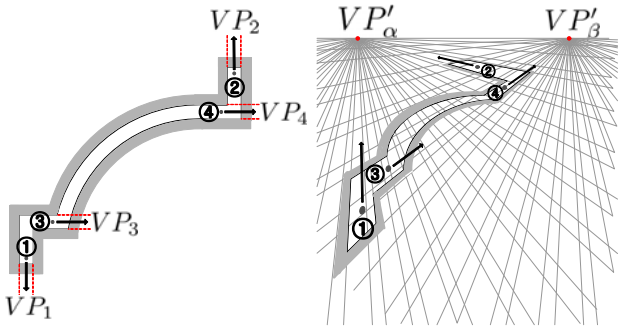

(a) (b)

Fig. 3. Effects of the projective transformation: (a) a loop-less environment with curved corridors and (b) the map after a projective transformation.

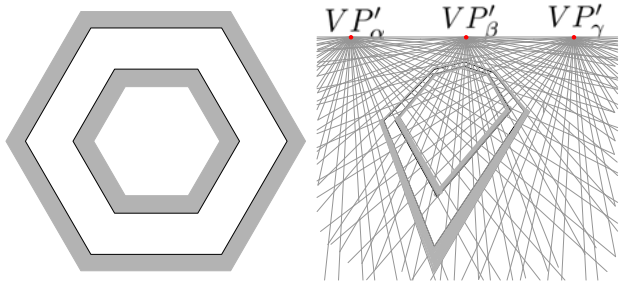

(a) (b)

Fig. 4. A hexagon-like building in (a) has only 3 $VP's$ as in (b).

closing cannot be applied for) which contains curved corridor (thus constraints cannot be assigned) as in Fig. 3(a). Then we have a projected map as in Fig. 3(b) where the vanishing points in the same direction are mapped into the same points: $VP_1 \& VP_2 \rightarrow VP'_\alpha$ and $VP_3 \& VP_4 \rightarrow VP'_\beta$.

These vanishing points after a projective transformation (VP' in short) are similar to the absolute landmark in the following aspects. First, one VP' is observed at different places (similar to omni-presence). For example, VP'_α is observed at ① and ② in Fig. 3(b) and the uncertainty of angle error at ② is reduced to that of ①. Thus the merit of the loop-closing is achieved in a loop-less map.

Second, the VP' can be accurately detected (similar to high accuracy). With the aid of the laser scanner, two line equations and a corresponding VP' can be accurately detected.

Third, the $VP's$ are sparse enough and thus possibility of a false data-association is low (similar to sparseness). In a typical indoor buildings, the corridors are designed along a few major directions. For example, a hexagon-like building (Fig. 4(a)) has only 3 $VP's$ whose angle differences are approximately $60°$, and thus a reliable data-association can be achieved.

Vanishing point in robot navigation has been studied by many researchers [6], [7]. [6] exploited artificial landmarks for the navigation and [7] used the vanishing point not to solve the SLAM problems but to control angular velocity.

The VPass is implemented in an EKF SLAM algorithm that estimates the heading angle of the robot while utilizing a VP' as landmarks. The major advantage of the VPass is that it can be used as an algorithmic sensor without artificial landmarks as used in [6]. In other words, it can be appended upon many existing navigation algorithms. The only required change is to extract the heading information not from the previous algorithm but from the VPass.

Experimental results show that by adding the VPass to the previous SLAM algorithm, a loop closing effect is achieved for a loop-less map.

This paper is organized as follows. In section II, several characteristics of vanishing points are explained. We modify the vanishing point to represent it in linear forms in section III. Section IV provides algorithm details. Experimental results are given in section V and conclusion follows.

II. Vanishing Point

For two parallel lines (line 1: $ax + by + c_1 = 0$, line 2: $ax + by + c_2 = 0$), the vanishing point is defined as an intersection point in the homogeneous coordinate as,

$$VP = \begin{bmatrix} a \\ b \\ c_1 \end{bmatrix} \times \begin{bmatrix} a \\ b \\ c_2 \end{bmatrix} = (c_2 - c_1) \begin{bmatrix} b \\ -a \\ 0 \end{bmatrix}. \quad (1)$$

For a fixed direction of the parallel lines (*i.e.* fixed a and b), there exist infinite VPs as $(c_2 - c_1)$ varies. Thus they cannot be a candidate of the absolute landmark.

However, if we apply for a projective transformation, all VPs for a fixed direction is mapped into the same point (Fig. 3(b)). Let us define a projective matrix (H_p) as,

$$H_p = \begin{bmatrix} p_1 & p_2 & t_x \\ p_3 & p_4 & t_y \\ v_1 & v_2 & 1 \end{bmatrix}, \quad (2)$$

where $\begin{bmatrix} p_1 & p_2 \\ p_3 & p_4 \end{bmatrix}$ is a non-singular matrix, $\begin{bmatrix} t_x & t_y \end{bmatrix}$ are translations along x and y directions, and $\begin{bmatrix} v_1 & v_2 \end{bmatrix}$ are projective coefficients. With this H_p, all VPs are mapped into one VP' as

$$VP' = H_p \times VP = (c_2 - c_1) \begin{bmatrix} bp_1 - ap_2 \\ bp_3 - ap_4 \\ bv_1 - av_2 \end{bmatrix}. \quad (3)$$

If we represent them in the non-homogeneous coordinate,

$$VP' = \begin{bmatrix} \frac{bp_1 - ap_2}{bv_1 - av_2} \\ \\ \frac{bp_3 - ap_4}{bv_1 - av_2} \end{bmatrix}, \quad (4)$$

which is independent of c_1 and c_2.

As it is addressed in the introduction, VP' is similar to the absolute in three aspects. First, one VP' is observed in different places far apart (similar to omni-presence). Second, the VP' can be accurately detected (similar to high accuracy). Third, the $VP's$ are sparse enough and thus possibility of a false data-association is low (similar to sparseness). But, VP'

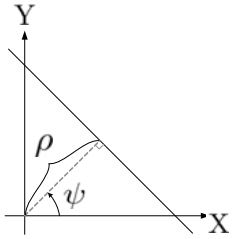

Fig. 5. Representation of a line by the shortest distance (ρ) and the normal angle (ψ).

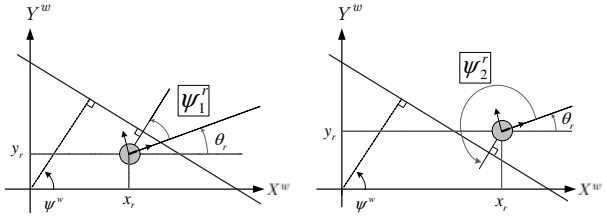

(a) (b)

Fig. 6. A line is represented by two different angles with respect to the robot's coordinate according to the position of robot.

itself is not adequate to be used for as landmarks because H_p is basically a nonlinear mapping. Thus, if we use VP' as landmarks, we cannot be free from the linearization errors. To get a linear form, we modify VP' in the next section.

III. Translation-Invariant Angle

To successfully work out VPAss algorithm in the EKF SLAM, we need to modify the VP' which is inherently a nonlinear mapping for the better performance.

Intuitively, it seems like that the normal angle of a line (ψ in Fig. 5) has the same meaning with the VP'. However, ψ cannot be used for because it has two major defects.

First, its relationship with the states of the robot is still nonlinear and thus the covariance of ψ is affected by the linearization errors. Let us represent a line by the shortest distance (ρ) and the normal angle (ψ). Also, let us use a superscript w and r to denote the base coordinate of the world and the robot, respectively. Then a sensor measurement z is the normal angle of a line with respect to the robot's coordinate (ψ^r) and it is a nonlinear function of a robot posture $\begin{bmatrix} x_r & y_r & \theta_r \end{bmatrix}^T$. And the normal angle with respect to the world's coordinate (ψ^w) can be written as follows:

$$z = \psi^r = atan2(dy, dx) - \theta_r, \tag{5}$$

where $dx = (\rho^w - x_r \cos\psi^w - y_r \sin\psi^w)\cos\psi^w$ and $dy = (\rho^w - x_r \cos\psi^w - y_r \sin\psi^w)\sin\psi^w$.[1]

Second, ψ^r is related to the position of robot and thus the covariance of ψ^r is affected by that of the robot position. Evidently, this is not the characteristic of the VP' because vanishing points are only related to the heading angle of the robot. This dependency can be identified in Fig. 6 where a line is represented by two different angles with respect to the robot's coordinate ($\psi_1^r = \psi_2^r + \pi$) according to the position of robot.

This dependency can be identified in equation, too. The covariance of ψ^r is the right-bottom scalar of the covariance of $\begin{bmatrix} \rho^r & \psi^r \end{bmatrix}^T$. This covariance (denoted by P_l^r) is given by,

$$P_l^r = J_r P_r J_r^T + J_l P_l^w J_l^T + R, \tag{6}$$

[1]Note that $\psi^r \neq atan(\tan\psi^w) - \theta_r = \psi^w - \theta_r$ for it is related to the position of the robot.

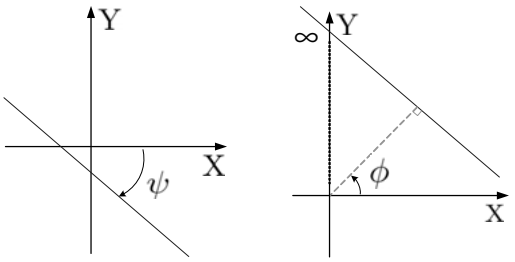

(a) (b)

Fig. 7. Definition of the TI-angle: (a) original line and (b) a line translated by $+\infty$ along y-direction.

where P_r is a covariance matrix of the robot state $\begin{bmatrix} x_r & y_r & \theta_r \end{bmatrix}^T$, P_l^w is a covariance matrix of line parameters $\begin{bmatrix} \rho^w & \psi^w \end{bmatrix}^T$, R is a measurement covariance, and J_r, J_l are Jacobians with respect to $\begin{bmatrix} x_r & y_r & \theta_r \end{bmatrix}^T$ and $\begin{bmatrix} \rho^w & \psi^w \end{bmatrix}^T$. In (6), it is evident that the covariance of ψ^r is affected by that of the robot position (P_r).

Instead of the normal angle (ψ), we propose '*a translation-invariant angle*' (ϕ, TI-angle in short) which is not affected by the robot position and has a linear relationship with the robot state. The TI-angle is the normal angle of a line translated by $+\infty$ along y-direction (Fig. 7). By this translation, ϕ is bounded in the range of $0 \leq \phi < \pi$.

Now let us use ϕ^w as a landmark and ψ^r as a measurement. Then the state is represented by $\begin{bmatrix} \theta_r & \phi_1^w & \cdots & \phi_m^w \end{bmatrix}^T$ (where m is the number of landmarks) and the equation of measurement expectation is represented in a linear form as follows:

Measurement expectation

Step 1)

For given states of θ_r and ϕ^w, take two candidates of measurement expectations as $\hat{\psi}_1^r = \phi^w - \theta_r$ and $\hat{\psi}_2^r = \phi^w - \theta_r + \pi$.

Step 2)

For a given real measurement ψ^r, the measurement expectation is given by $\hat{z} = \underset{\hat{\psi}_i^r, i=1,2}{argmax}(\cos(\psi^r - \hat{\psi}_i^r))$, where ψ^r is the real measurement.

Step 3)

The covariance of $\hat{z}$ is given by $cov(\hat{z}) = cov(\phi^w) + cov(\theta_r)$, where $cov(\cdot)$ denotes for the covariance.

Note that both $\hat{z}$ and $cov(\hat{z})$ is not related to the robot position and there is no linearization process.

IV. Algorithm Details

For the implementation of the VPass, we adopted the EKF SLAM framework as follows

Step 1) Initialization

Initialize state X and covariance P by $X(1) = \theta_r(1)$ and $P(1) = cov(\theta_r(1))$.

Step 2) Predict

For a given angular velocity (ω) and a sampling period (Δt),

$$\begin{aligned} X(k+1) &= FX(k) + G\omega + v, \\ P(k+1) &= FP(k)F^T + Q, \end{aligned} \tag{7}$$

where $F = I_{(m+1)\times(m+1)}$, $G = \begin{bmatrix} \Delta t \\ \oslash_{m\times 1} \end{bmatrix}$, $v = \begin{bmatrix} v_1 \\ \oslash_{m\times 1} \end{bmatrix}$, $Q = \begin{bmatrix} \sigma_v^2 & \oslash_{1\times m} \\ \oslash_{m\times 1} & \oslash_{m\times m} \end{bmatrix}$ with $v_1 \sim \mathcal{N}(0, \sigma_v^2)$.

Step 3) Measurement of normal angles of lines

Using the laser scanner, detect a distinctive lines around the robot to extract normal angles ψ_i^r.

Step 4) Perform the data-association

For each measurement of ψ_i^r, perform the data-association using the innovation of $\psi_i^r - \hat{z}$ where $\hat{z}$ is given by the equation of the measurement expectation in the previous section.

Step 5) Update

Update the state and covariance by using the EKF algorithm.

Step 6) Landmark augmentation

If there is ψ_i^r that is expected to be a new landmark, find the TI-angle of the landmark with respect to the world coordinate (ϕ_i^w). Then append ϕ_i^w at the end of the state X and update the covariance P as follows.

$$X'(k) = \begin{bmatrix} X(k) \\ \phi_i^w \end{bmatrix},$$

$$P'(k) = \begin{bmatrix} cov(\theta_r) & cov(\theta_r, \phi^w) & cov(\theta_r, \phi_i^w) \\ cov(\phi^w, \theta_r) & cov(\phi^w) & cov(\phi^w, \phi_i^w) \\ cov(\phi_i^w, \theta_r) & cov(\phi_i^w, \phi^w) & cov(\phi_i^w) \end{bmatrix},$$

where $cov(\theta_r, \phi^w)$ is a covariance between θ_r and landmarks already registered. Note that $cov(\phi_i^w)$ can be acquired by the procedures in the previous section and that $P(k) = \begin{bmatrix} cov(\theta_r) & cov(\theta_r, \phi^w) \\ cov(\phi^w, \theta_r) & cov(\phi^w) \end{bmatrix}$.

Step 7) Use of the VPass information

Use of $X_1(k) = \theta_r(k)$ as a corrected angle.

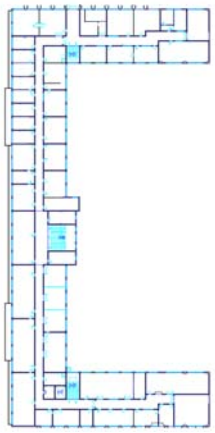

Fig. 8. CAD drawing of an indoor building without a loop.

Step 8) Repeat 2-7

V. Experimental Results

We conducted two sets of off-line experiments. In other words, we saved all the sensor information and applied for various algorithms in off-line. Firstly, we performed SLAMs for a long corridor environment without loop whose CAD drawing is shown in Fig. 8. A pioneer mobile robot equipped with one laser scanner was used for in a speed of $0.3m/sec$ at a control frequency of $4Hz$. The total travel length was $180.7m$. Fig. 9 shows the grid maps generated by odometry, line-based EKF SLAM [8]–[10], and a line-based EKF SLAM with the VPass. From these figures, we can verify that the line-based EKF with the VPass yields the best-matched map.

With this result, let us explain in-depth operations of the VPass. Initially, TI-angles of two lines A and B in Fig. 10(a) are registered as new landmarks. At step 660, the line C is being detected with high angle uncertainty and it is data-associated to the TI-angle of the line B. The angle uncertainty of the line C is reduced to that of the line B, and this brings forth the similar effects of the loop-closing. By virtue of the small TI-angle uncertainty of the line C, the orthogonality of corridors 1 and 2 is well preserved. Similar phenomenon occurs when the robot detects a line D at step 2200. The high angle uncertainty of the line D is reduced to that of A by data-association.

Note that the corridor 2 in Fig. 9(c) is not linear compared to that of the line-based EKF SLAM (Fig. 9(b)). This phenomenon was induced because we assigned a relatively large value of measurement uncertainty for the robust data-association. We were able to do that for the TI-angles are sparse enough (in this building, they are separated by 90°), and this is one of the advantages of the VPass.

Secondly, we conducted another set of experiments for an indoor building with one large loop (Fig. 11). The same robot was used for and the travel length was $197.5m$. During the experiment, a significant rotational error had occurred at the

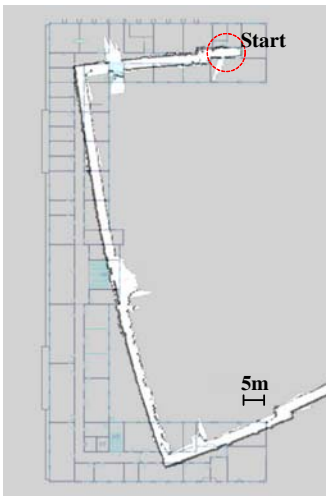

(a)

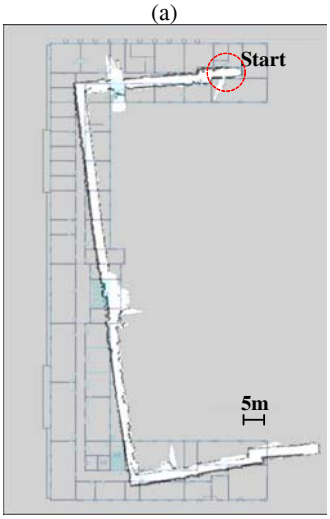

(b)

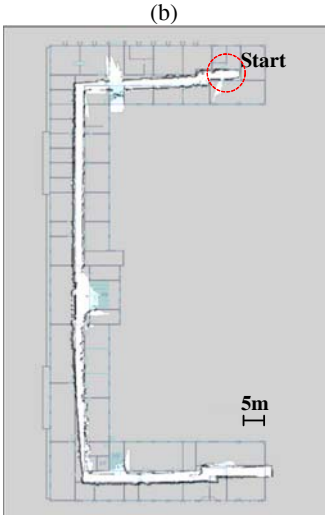

(c)

Fig. 9. Experimental results: (a) odometry map, (b) a line-based EKF SLAM map, and (c) a line-based EKF SLAM map with VPass.

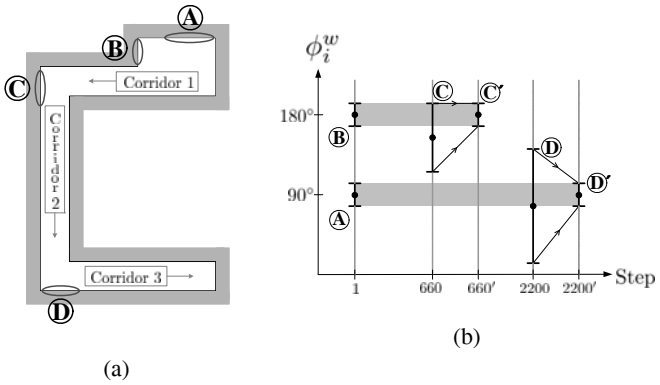

(a) (b)

Fig. 10. Description of in-depth operations of the VPass: (a) an exaggerated map of the building and (b) the registered landmarks according to the time steps. Initially, TI-angles of two lines A and B in (a) are registered as new landmarks. At step 660, the line C is being detected with high angle uncertainty and it is data-associated to the TI-angle of the line B. The angle uncertainty of the line C is reduced to that of the line B, and this brings forth the similar effects of the loop-closing. By virtue of the small TI-angle uncertainty of the line C, the orthogonality of corridors 1 and 2 is well preserved. Similar phenomenon occurs when the robot detects a line D at step 2200. The high angle uncertainty of the line D is reduced to that of A by data-association.

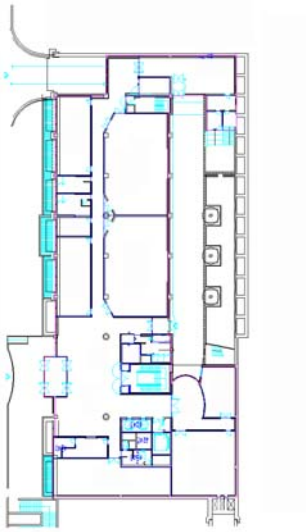

Fig. 11. CAD drawing of an indoor building with a loop.

point A and the line-based EKF SLAM could not be able to recover it. By this reason, the maps from the odometry (Fig. 12(a)) and from the line-based EKF SLAM (Fig. 12(b)) show similar poor matching performances. However, by the virtue of the VPass, the errors were compensated for and we were able to get an accurate map as shown in Fig. 12(c).

VI. Conclusion and Remarks

In this paper, we proposed an algorithmic compass that yields the heading information of a mobile robot using vanishing points in indoor environments: VPass. The VPass is an EKF SLAM algorithm that estimates the heading angle of the robot while utilizing a Translation-Invariant angle (TI-angle) of lines as landmarks.

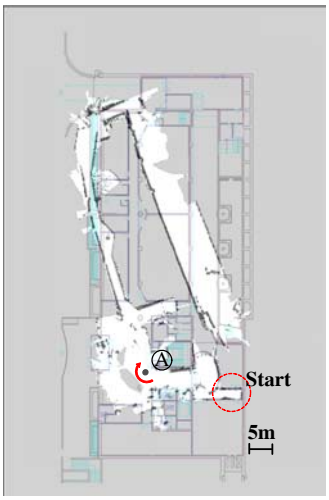

(a)

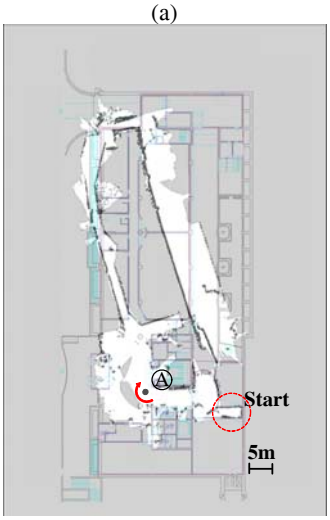

(b)

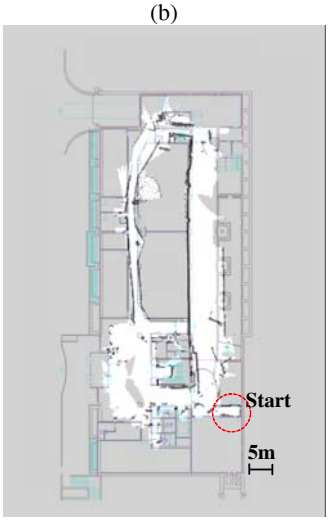

(c)

Fig. 12. Experimental results: (a) odometry map, (b) a line-based EKF SLAM map, and (c) a line-based EKF SLAM map with VPass.

The TI-angle has the following beneficial features. First, it is observed in different places far apart. Second, it can be accurately detected. Third, they are sparse enough and thus a robust data-association can be achieved.

By these virtues of the TI-angle, the VPass yields an accurate heading information and enables a loop-closing effect (which is a significant reduction of errors by revisiting a known place through a loop) even for a loop-less map. Experimental results for paths around $200m$ show that the VPass enhances the performance of previous SLAM algorithms.

Three remarks should be mentioned. First, the VPass is based on the EKF framework which is apt to diverge by a false data-association. Thus, we need to analyze the sensitivity of the data-association according to the changes of the measurement covariance. Second, at this time, only the information of the heading angle is used. We believe that the covariance of the angle will be also useful and will develop related equations in the near future. Third, for the validation of robustness, we are planning to perform sonar-sensor based experiments for a nested-loops environments.

VII. ACKNOWLEDGMENTS

This paper was supported by multiple funds of Human Resource Development Program (MKE), UTRC program (ADD), Network-Based Humanoid program (KIST), SMBA program, 06-UACT program (KICTEP), and KRF-2008-313-D00400.

REFERENCES

[1] N. L. Doh, H. Choset, and W. K. Chung, "Relative localization using path odometry information," *Autonomous Robot*, vol. 21, no. 2, pp. 143–154, 2006.

[2] S. Julier, J. Uhlmann, and H. F. Durrant-Whyte, "A new method for the nonlinear transformation of means and covariances in filters and estimators," *IEEE Trans. on Automatic Control*, vol. 45, no. 3, pp. 477–482, 2000.

[3] C. Stachniss, D. Hähnel, and W. Burgard, "Exploration with active loop-closing for fastSLAM," in *Proc. of IEEE/RSJ Int. Conf. on Intelligent Robots and Systems*, vol. 2, pp. 1505–1510.

[4] P. Jensfelt, H. I. Christensen, and G. Zunino, "Integrated systems for mapping and localization," in *International Conference on Robotics and Automation Workshop*, 2002.

[5] V. Nguyen, A. Harati, A. Martinelli, and R. Siegwart, "Orthogonal SLAM: a step toward lightweight indoor autonomous navigation," in *Proc. of IEEE/RSJ Int. Conf. on Intelligent Robots and Systems*, pp. 5007–5012, 2006.

[6] G. Garibotto, M. Ilic, and S. Masciangelo, "Vision-based based navigation in service robotics," *Lecture Notes in Computer Science*, vol. 974, pp. 313–318, 1995.

[7] R. F. Vassallo and J. Santos-Victor, "A purposive strategy for visual-based navigation of a mobile robot," in *Proceedings of Midwest Symposium on Circuits and Systems*, pp. 334–337.

[8] Y.-H. Choi, T.-K. Lee, and S.-Y. Oh, "A line feature based SLAM with low grade range sensors using geometric constraints and active exploration for mobile robot," *Autonomous Robot*, vol. 24, no. 1, pp. 13–27, 2008.

[9] D. C. Yuen and B. A. MacDonald, "Line-based SMC SLAM method in environment with polygonal obstacles," in *Australasian Conference on Robotics and Automation*, 2003.

[10] A. Garulli, A. Giannitrapani, A. Rossi, and A. Vicino, "Mobile robot SLAM for line-based environment representation," in *Decision and Control,2005 and 2005 European Control Conference*, pp. 2041–2046, 2005.